Ann. Geophys., 25, 855–861, 2007
www.ann-geophys.net/25/855/2007/

Annales Geophysicae

On the seasonal variations of the threshold height for the occurrence of equatorial spread F during solar minimum and maximum years

G. Manju, C. V. Devasia, and R. Sridharan

Space Physics Laboratory, Vikram Sarabhai Space Centre, Trivandrum – 695 022, Kerala, India

Received: 16 June 2006 – Revised: 7 March 2007 – Accepted: 20 March 2007 – Published: 8 May 2007

Abstract. A study has been carried out on the occurrence of bottom side equatorial spread F (ESF) and its dependence on the polarity and magnitude of the thermospheric meridional wind just prior to ESF occurrence during summer, winter and equinox seasons of solar maximum (2002) and minimum years (1995), using ionosonde data of Trivandrum (8.5° N, 76.5° E, dip=0.5° N) and SHAR (13.7° N, 80.2° E, dip ∼5.5° N) in the Indian longitude sector. In this study, we have examined the changes in the threshold height of the base of the F layer for the triggering of ESF, irrespective of the magnitude and polarity of the meridional winds during the above periods. The study indicates that the threshold height above which ESF triggering is entirely controlled only by the collisional R-T instability is least for summer months, with higher values for winter and equinox, during the solar minimum period, whereas for the solar maximum period the threshold height is least for winter, with higher values for summer and equinox. But the range over which the threshold height varies is very narrow (<15 km) for solar minimum in relation to the large range of variation (>50 km) in the solar maximum epoch. Further to this, the study also reveals a clear-cut increase in threshold height with solar activity for all seasons. Clear-cut seasonal variability is also observed in the threshold height, especially for solar maximum. The study quantifies the level of the base of the F layer below which neutral dynamical effects play a decisive role in the triggering of ESF during different seasons and solar epochs.

Keywords. Ionosphere (Equatorial ionosphere; Ionospheric irregularities; Plasma waves and instabilities)

Correspondence to: G. Manju
(manju_spl@vssc.gov.in)

1 Introduction

Equatorial Spread F (ESF) irregularities are night-time plasma density irregularities of scale sizes ranging from centimetres to several hundred kilometres (Farley et al., 1970; Ossakow, 1981; Woodman and La Hoz, 1976; Fejer and Kelly, 1980; Abdu et al., 1981; Fejer et al., 1999, Hysell and Burcham, 2000). The primary process responsible for the generation of these irregularities is the Collisional Raleigh-Taylor (CRT) instability mechanism operating in the post sunset bottom side F region (Haerendel, 1974; Costa and Kelley, 1978). Equatorial spread F occurrence shows large day-to-day, seasonal, longitude, solar cycle, and magnetic activity variabilities (Chandra and Rastogi, 1970; Kelley and McClure, 1981; Abdu et al., 1981, Huang et al., 1987; Sahai et al., 2000, Abdu, 2001,Tsunoda, 1985). The effects of meridional winds, which move plasma along field lines both vertically and horizontally, have been examined by some workers (Maruyama and Matuura, 1984; Maruyama, 1988). Studies on the role of seed perturbations in the generation of F region irregularities have been reported by Whitehead (1971) and Fejer et al. (1999). One of the important factors that could contribute to the ESF day-to-day variability is the thermospheric meridional/transequatorial wind that would cause an asymmetry in the equatorial anomaly, increase the E region conductivity and load the F region dynamo, thus limiting the post sunset F region height rise. The increased ion-neutral collision frequency (ν_{in}) at lower heights causes reduction in the linear growth rate of the R-T mechanism responsible for the generation of ESF irregularities (Maruyama, 1988; Mendillo, 1992). Devasia et al. (2002) showed that converging/diverging thermospheric meridional winds become significant with the equatorward wind being present when $h'F$ was below a threshold height ($h'F_c$), for the R-T instability to become triggered. Above the critical height the polarity did not matter. This threshold height of $h'F$ (defined by them) has been found to be

Published by Copernicus GmbH on behalf of the European Geosciences Union.

~300 km for the occurrence of ESF during equinoctial periods and showed a linear solar activity dependence (Devasia et al., 2002; Jyoti et al., 2004). Raghavarao et al. (1993) conjectured that such equatorward winds could be produced as a result of the pressure bulges associated with Equatorial Temperature and Wind Anomaly (ETWA). The present study aims at examining the seasonal variation of $h'F_c$ during solar minimum and maximum epochs with a view to unravel the enigmatic day-to-day variability of the ESF occurrence during a particular season.

2 Experimental set up and data and method of analysis

Ionosonde data, of Trivandrum (8.5° N, 76.5° E, dip latitude 0.5° N) and SHAR (13.7° N, 80.2° E, dip latitude 5.5° N) in the Indian longitude sector, have been made use of in this study. Data corresponding to the ESF occurrence in the summer, winter and equinox seasons of 1995 (solar minimum) and 2002 (solar maximum) have been examined. The $h'F$ and meridional wind values just prior to the triggering of ESF are obtained for each day during these seasons. The method given by Krishna Murthy et al. (1990) is used for estimating the meridional winds. In this method, the vertical drift of the evening F layer is estimated for the two stations (Trivandrum and SHAR), accounting for the effects due to recombination and diffusion. The F-region vertical drift at the magnetic equator over Trivandrum is purely electrodynamical in nature while that at a low-latitude station, like SHAR, has a contribution from the meridional winds (U) in addition to diffusion along the magnetic field lines. The observed vertical drift velocities (V_o) are initially derived from the rate of change of $h'F$ (d($h'F$)/dt). The true vertical drift is obtained from V_d=V_o−βH, where β is the effective recombination coefficient and H is the scale height given by H=(1/N dN/dh)$^{-1}$. N is the electron density and βH is the correction due to recombination.

The actual meridional wind for the period 18:00–06:00 h is estimated from the equations for the vertical drift at the two stations as:

$$\mathbf{U} = [2(\mathbf{V}_D \cos \mathbf{I} - \mathbf{V})/\sin 2\mathbf{I}] - \mathbf{W}_D \tan \mathbf{I}, \quad (1)$$

where $\mathbf{V}_D$ is the vertical drift over Trivandrum and $\mathbf{V}$ that over SHAR. $\mathbf{I}$ is the dip angle at SHAR and $\mathbf{W}_D$ the plasma drift velocity due to plasma diffusion and is given by $\mathbf{g}/\nu_{in}$, where $\mathbf{g}$ is the acceleration due to gravity and ν_{in} is the ion-neutral collision frequency. The error in the meridional wind estimation using this method is estimated to be about $\pm 25\,\mathrm{ms}^{-1}$ (Krishna Murthy et al., 1990). The meridional wind velocities corresponding to the post-sunset F-region heights ($h'F$ at Trivandrum), just before the onset of each of the ESF events, have been obtained for the different seasons corresponding to the solar minimum and maximum periods considered for the present study. Only those events for which ESF is triggered before 20:00 IST are considered for this study. As mentioned earlier, the criterion of ESF occurrence irrespective of the polarity of meridional winds is applied to $h'F$ to determine the threshold height $h'F_c$ below which equatorward wind is essential for the triggering of ESF (Devasia et al., 2002; Jyoti et al., 2004).

3 Results

Figure 1a shows the scatter plot of the meridional wind velocities against $h'F$ values of each of the ESF events during the summer solstice of solar minimum (left panel) and solar maximum (right panel) periods. It may be noted that the wind magnitudes show large variabilities during the solar maximum period in comparison to the solar minimum period and the $h'F$ values also show large variability (250–375 km), unlike those during the solar minimum period where they are limited to a narrow range of 225–250 km. The threshold height level is indicated in all the scatter plots by the dashed lines. It should be noted that the $h'F_c$ could be unambiguously determined for the solar maximum summer months while for other cases only the upper limit of $h'F_c$ could be identified. It is clearly seen that the threshold height for the summer solstice increases from 228 km at solar minimum to 314 km at solar maximum. Figure 1b depicts the scatter plot of the meridional wind vs. $h'F$ at 19:00 IST on the non-spread F days (for which data were available) during the summer of solar maximum. It is seen that out of the 7 days, for four of the days, the meridional wind is clearly poleward, as expected when the $h'F$ is below the threshold level. For the other three days, the meridional wind is equatorward. On one of these three days the $h'F$ is just above the threshold making it an exception. It is likely that the seed perturbations which are assumed to be omnipresent might not be of sufficient amplitude for an ESF occurrence on that day. For the other two days, the $h'F$ is clearly below the threshold level and the wind is equatorward. Again, the lesser magnitude of the seed perturbations is believed to be the reason for the non-occurrence of ESF on these two days.

Figure 2 shows the scatter plot of the meridional wind velocities and $h'F$ values for winter solstice of solar minimum (left panel) and solar maximum (right panel). The variabilities in $h'F$ during winter solstice periods are very large in comparison to those observed in summer of both solar minimum and maximum epochs. Another important observation during solar maximum is that meridional winds during the winter solstice period are in general poleward, whereas during summer solstice they are predominantly equatorward. In general, these patterns are expected to be so, based on the sub-solar points for thermospheric heating, for the different seasons. But the ETWA- related meridional winds, which follow the day-to-day variability of the EIA, modulate the inter-hemispheric winds and thereby result in higher or lower values of meridional winds either poleward or equatorward (depending on the magnitude and direction of the

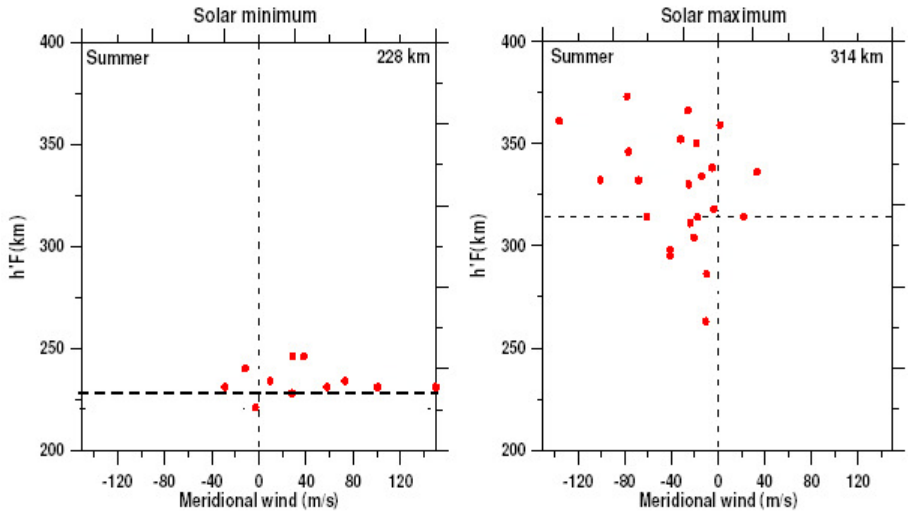

Fig. 1a. Scatter plot of meridional wind and $h'F$ prior to triggering of ESF for summer solstice of solar minimum (left panel) and solar maximum (right panel).

ETWA related winds). For the winter solstice, the upper bound (Jyoti et al., 2004) of the threshold height could only be delineated and it was found to increase from 240 km at solar minimum to 264 km at solar maximum. It is seen that the threshold height shows an increase with solar activity for winter solstice similar to the summer solstice, but to a significantly lesser extent.

Figure 3 depicts the scatter plot of the meridional wind velocities and $h'F$ values for equinox of solar minimum (left panel) and solar maximum (right panel). As is seen from the figure for solar minimum, the upper bound of the threshold height could only be identified with the available database. Nevertheless, the increase in the threshold height from 243 km (upper bound) at solar minimum to 305 km at solar maximum is clearly discernible. Interestingly, the meridional wind values, during the equinox of solar maximum, reveal an almost equal distribution of values in the poleward and equatorward directions, indicating a clear-cut transition from the summer to the winter pattern.

Figure 4 (dashed curve) shows the seasonal variation in the threshold height for the solar minimum epoch, essentially redrawn from the earlier figure showing the nature of the variation starting from the summer solstice to the equinox and then to the winter solstice. The threshold height is 228 km for summer, while the upper bounds are 243 km and 240 km for the equinox and winter, respectively. It shows a fairly smooth variation over a span of 15 km. This result suggests nearly the same probability of occurrence of ESF throughout the solar minimum period, as the threshold height is seen to be confined to 228–243 km. Unlike this, the seasonal variation of the threshold height during the solar maximum period is quite significant. The threshold height (for solar maximum) is found to be 264 km (upper bound) for winter, with

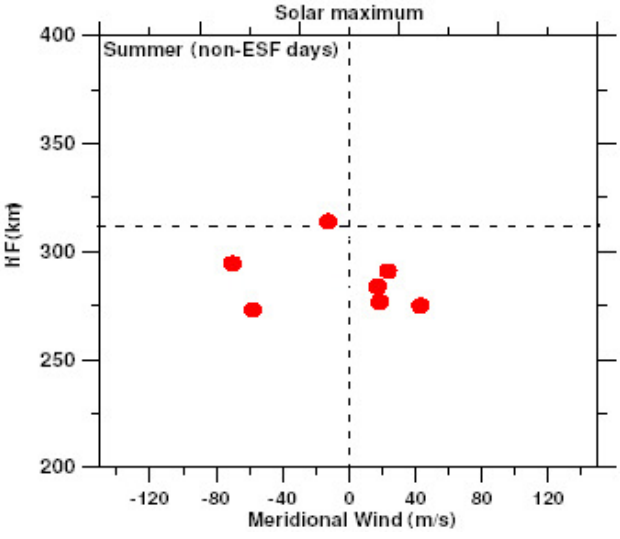

Fig. 1b. Scatter plot of meridional wind and $h'F$ at 19:00 h on non-ESF days for summer solstice of solar maximum.

increased values of 305 km and 314 km for the equinox and summer, respectively.

It is accepted that the phenomenon of ESF is a result of a hierarchy of multistep, nonlocal plasma processes involving the collisional and collision-less Rayleigh-Taylor and $\boldsymbol{E}\times\boldsymbol{B}$ instabilities and drift waves driven by coupled electrodynamic and neutral atmospheric processes (Haerendel, 1973; Ossakow, 1981; Zalesak et al., 1982; Sekar and Kelley, 1998; Basu and Coppi, 1999). However, the primary process responsible for the generation of large-scale ESF irregularities is the collisional Rayleigh-Taylor (CRT) instability

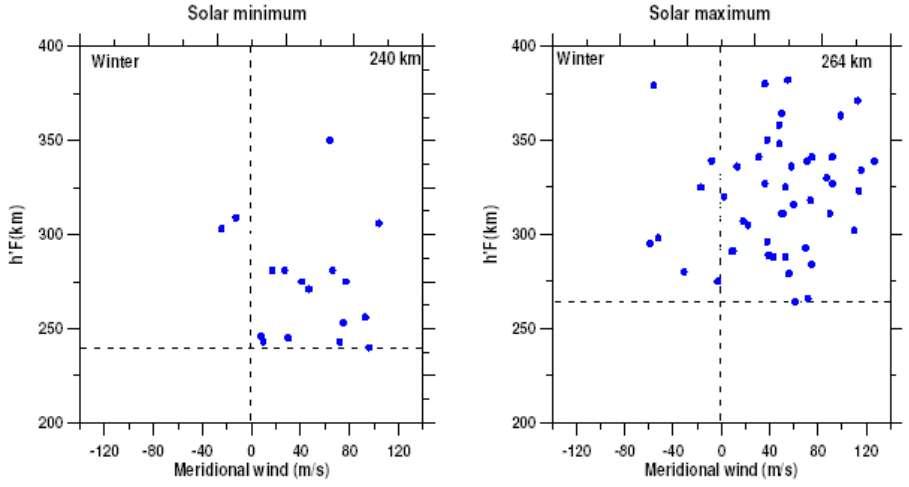

Fig. 2. Scatter plot of meridional wind and $h'F$ prior to triggering of ESF for winter solstice of solar minimum (left panel) and solar maximum (right panel).

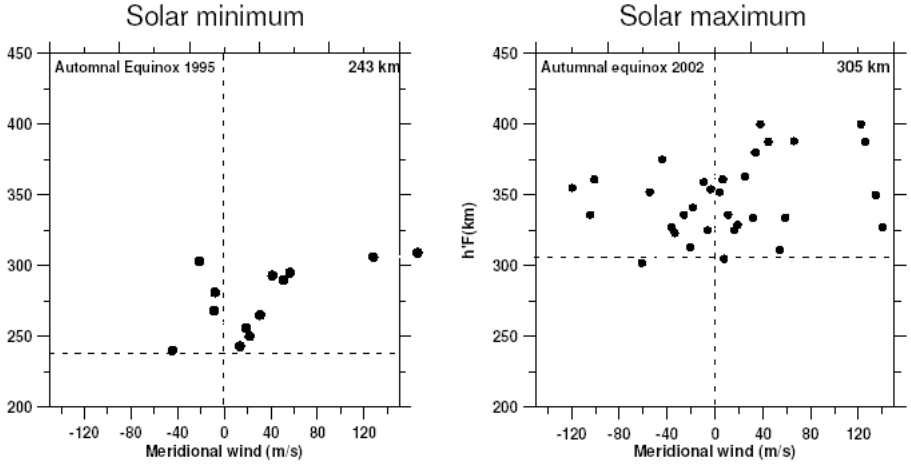

Fig. 3. Scatter plot of meridional wind and $h'F$ prior to triggering of ESF for equinox of solar minimum (left panel) and solar maximum (right panel).

mechanism, which operates in the post- sunset bottomside F region under certain favourable conditions. When the conditions are not favourable for the instability to trigger ESF, factors like neutral winds could also contribute to it. With the delineation of a seasonally varying threshold height for triggering of ESF irrespective of the magnitude and polarity of the meridional winds, which at the point of convergence (i.e. over the dip equator) manifest as vertically downward winds, the triggering of an ESF on a particular day (when the F layer is at or above the threshold height) can be entirely attributed to the collisional Rayleigh-Taylor (CRT) instability mechanism.

The expression for the growth rate of the generalized R-T instability in terms of different forcing parameters is given as (Sekar and Raghavarao, 1987; Kelly, 1989)

$$\gamma = 1/L[g/\nu_{in} + \mathbf{E}_x/\mathbf{B} + \mathbf{W}_x(\nu_{in}/\Omega_i) - \mathbf{W}_z], \quad (2)$$

where $\mathbf{E}_x$ is the zonal electric field, $\mathbf{B}$ is the geomagnetic field, ν_{in} is the ion-neutral collision frequency, Ω_i is the gyrofrequency, $\mathbf{W}_x$ and $\mathbf{W}_z$ are the zonal and vertical winds, respectively. The role of the electric fields and zonal winds is twofold; they dictate the level of $h'F$ where the gravity would be the dominant driving force in the presence of a steep bottom side gradient and they also contribute to the growth of the instability through Eq. (2), the latter being only secondary. On the other hand, the role of a vertically downward wind would be equivalent to the primary driving force viz. gravity, in generating the polarization field. Sekar and Raghavarao (1987) have made a comparative estimate of the effect of vertical winds and gravity and arrived at a

conclusion that at ∼300 km a vertical wind magnitude of 20 ms^{-1} would be as effective as gravity itself. The crux of the matter, in the present paper, is that above the newly-defined threshold height ($h'F_c$), the growth rate is mainly controlled by ν_{in} and L while E_x and W_x could be modulating factors.

4 Discussion

The above characteristics related to the variations of the critical height, seem to originate from the linkage between the Equatorial ionisation anomaly (EIA) and ESF, providing an implicit control of the meridional wind on ESF. Maruyamma and Matuura (1984) suggested a mechanism wherein strong meridional winds create a N-S asymmetry in the EIA, thus producing substantial changes in E-region integrated conductivities, which, in turn, control the post-sunset F-region height rise and the triggering of ESF. Raghavarao et al. (1988) experimentally showed the intensification of the crest-to-trough ratio of the EIA well in advance of the onset of ESF linking the EIA and the ESF. Following this, Sridharan et al. (1994) demonstrated the existence of a precursor in the OI 630 nm day glow that represented the EIA strength which facilitated the prediction of ESF at least 2 h prior to its actual occurrence. Further, Lee et al. (2005) have shown the linkage of seasonal ESF variability with EIA asymmetry. Devasia et al. (2002) have shown meridional winds to be the physical parameter connecting EIA and ESF. They suggested that the meridional winds were the outcome of the pressure bulges associated with ETWA (Raghavarao et al., 1993). Jyoti et al. (2004) brought out the dependence of the threshold height $h'F_c$, on solar activity for the equinox.

In the present study, the seasonal variation in the threshold height for the triggering of ESF has been examined, corresponding to the solar minimum and maximum phases. Three distinct seasons have brought out the representative characteristics of meridional winds in association with the ESF events.

The increased threshold height at solar maximum for all three seasons is possibly due to the increase in ion-neutral collision frequencies as a consequence of the increased concentration of neutrals at a given altitude. During periods of high solar activity, the scale height (H) of the neutrals in the F region changes significantly due to the increase in temperature (H=RT/Mg), where R is the gas constant, T is the temperature in °K, M is the molecular mass and g the acceleration due to gravity. The increase in H with increasing solar activity results in a swelling of the thermospheric neutral densities (Fuller-Rowell et al., 1996). As a result the ion-neutral collision frequencies would increase. This, in turn, would result in a reduced growth rate of the RT instability (Eq. 2) for a given altitude at solar maximum in comparison to that at solar minimum. Therefore the optimum growth

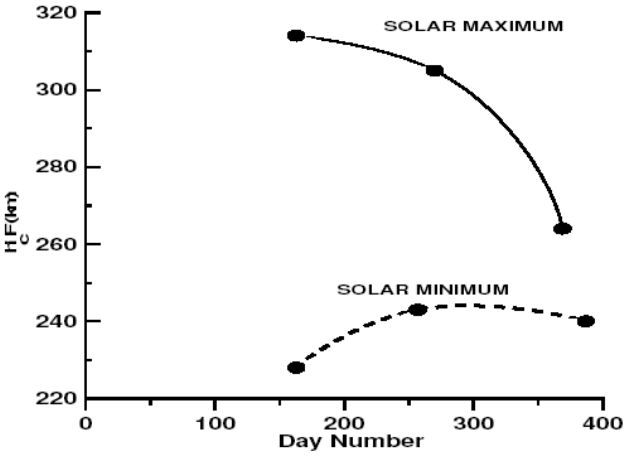

Fig. 4. The seasonal variation in threshold height for solar minimum (dashed) and maximum (solid) epoch.

rate, which results in ESF triggering, will be achieved only at a higher altitude in solar maximum.

There is a clear-cut seasonal variation in threshold height ($h'F_c$) for the solar maximum epoch, with $h'F_c$ being the highest for summer (314 km) and reducing towards equinox (305 km) and winter (264 km). In solar minimum the seasonal variation of $h'F_c$ is over a narrow range of ∼15 km, with the minimum occurring during summer. As already mentioned, $h'F_c$, being the F-region base height, above which the RT instability alone suffices for the triggering of ESF, shows sesonal variabilities, most likely caused by the parameters controlling the primary RT instability generation (1st term, Eq. 2) the combined effects of the seasonal variabilities in the gradient scale length (L) and ion-neutral collision frequency (ν_{in}) would modulate the growth rate of the RT instability seasonally. This would manifest as changes in the $h'F_c$level in such a way that the optimum growth rate of the RT instability is attained for different seasons. In this context, it is to be noted that the comparable values of $h'F_c$ during different seasons of solar minimum indicates nearly the same probability of occurrence of ESF when the base of the F-region is above the threshold level.

Another aspect of interest is that during solar maximum, the threshold height is minimum for winter in relation to the other two seasons, i.e. in winter (of solar maximum), the meridional winds have a role in ESF triggering only when the base of the F layer is below 264 km while for the other seasons, winds play a role when the base of the F layer is below 305 km (for equinox) and 314 km (for summer), respectively. This could as well be due to the seasonal variation of thermospheric temperatures and the associated enhancement of ion-neutral collision frequency, as in the case of the solar activity dependence. In the case of solar minimum the threshold height is minimum for summer in relation to the other two seasons, though the differences are only very marginal.

Thus, the minimum value of the threshold height undergoes significant changes from winter in solar maximum to summer in solar minimum, highlighting the complexities in the thermosphere-ionosphere system.

In the whole study, one of the important factors with regard to the RT instability, namely the seed perturbations, has been assumed to be omnipresent, which need not necessarily be true. It is generally believed that gravity waves, either in-situ generated or propagated from a different source region, could be the seed. Though the atmosphere sustains/supports gravity wave activity, they are bound to have their own characteristics and also forced variability. These would definitely modulate the triggering and evolution of the phenomenon. Though our comprehension on the background ionospheric and thermospheric conditions has significantly increased, there is a large gap with regard to the seed perturbations. The consistency of the results, with the assumption that the seed perturbations are always present appears to vindicate such an assumption. However, when we investigate on a case-by-case basis, unless the seed perturbations are also quantified, all the observations may not be explained. Concerted efforts have to be made in the future to address this problem.

5 Conclusions

The important conclusions of the present study are:

1. During solar minimum, the threshold height ($h'F_c$), above which ESF triggering is entirely controlled by the collisional R-T instability is least for summer, with relatively higher but comparable heights during for winter and autumnal equinox seasons. The range of seasonal variability of $h'F_c$ is rather small.

2. During solar maximum, the above threshold height is least for winter, with higher heights for summer and autumnal equinox seasons. The range of variability is rather large compared to solar minimum epoch.

3. Increase in threshold height with solar activity for all seasons is attributed to the increase in ν_{in}, that would result in a reduced growth rate of the RT instability for a given altitude at solar maximum in comparison to that at solar minimum.

Acknowledgements. Topical Editor M. Pinnock thanks B. V. Krishna Murthy and another referee for their help in evaluating this paper.

References

Abdu, M. A., Batista, I. S., and Bittencourt, J. A.: Some characteristics of spread F at the magnetic equatorial station Fortaleza, J. Geophys. Res., 86(A8), 6836–6842, 1981.

Abdul, M. A.: Outstanding problems in equatorial ionosphere-thermosphere electrodynamics relevant to spread F, J. Atmos. Sol. Terr. Phys., 63, 869–884, 2001.

Basu, B. and Coppi, B.: Relevance of plasma and neutral wind profiles to the topology and the excitation of modes for the onset of spread F, J. Geophys. Res., 104, 225–31, 1999.

Chandra, H. and Rastogi, R. G.: Solar cycle and seasonal variation of spread F near the magnetic equator, J. Atmos. Solar Terr. Phys., 32, 439–444, 1970.

Costa, E. and Kelley, M. C.: On the role of steepened structures and drift waves in equatorial spread F, J. Geophys. Res., 83, 4359–4364, 1978.

Devasia, C. V., Jyoti, N., Viswanathan, K. S., Subbarao, K. S. V., Tiwari, D., and Sridharan, R.: On the plausible linkage of thermospheric meridional winds with equatorial spread F, J. Atmos. Sol. Terr. Phys., 64, 1–12, 2002.

Farley, D. T., Balsley, B. B., Woodman, R. F., and McClure, J. P.: Equatorial spread F: Implications of VHF radar observations, J. Geophys. Res., 75, 7199–7216, 1970.

Fejer, B. G., Scheerliess, L., and de Paula, E. R.: Effects of the vertical plasma drift velocity on the generation and evolution of equatorial spread F, J. Geophys. Res., 104, 19 859–19 869, 1999.

Fejer, B. G. and Kelley, M. C.: Ionospheric irregularities, Rev. Geophys. Space Phys., 18, 401–454, 1980.

Fuller-Rowell, T. J., Codrescu, M. V., Moett, R. J., and Quegan, S.: On the seasonal response of the thermosphere and ionosphere to geomagnetic storms, J. Geophys. Res., 101, 2343–2353, 1996.

Haerendel, G.: Theory of equatorial spread F, Report, Max- Plank Inst. fur Phys. and Astrophys., Munich, 1974.

Huang, Y. N., Cheng, K., and Huang, W. T.: Seasonal and solar cycle variations of spread F at equatorial anomaly crest zone, J. Geomag. Geoelectr., 39, 639–657, 1987.

Hysell, D. L. and Burcham, J.: Ionospheric field estimates from radar observations of the equatorial electrojet, J. Geophys. Res., 105, 2443–2460, 2000.

Jyoti, N., Devasia, C. V., Sridharan, R., and Tiwari, D.: Threshold height ($h'F$c) for the meridional wind to play a deterministic role in the bottom side equatorial spread F and its dependence on solar activity, Geophys. Res. Lett., 31, L12809, doi:10.1029/2004GL019455, 2004.

Kelley, M. C. and McClure, J. P.: Equatorial spread-F: a review of recent experimental results, J. Atmos. Terr. Phys., 43, 427–435, 1981.

Kelly, M. C.: The Earth's ionosphere: Plasma physics and electrodynamics, Academic Press, San Diego, CA., 1989.

Krishna Murthy, B. V., Hari, S. S., and Somayajulu, V. V.: Nighttime equatorial thermospheric meridional winds from $h'F$ data, J. Geophys. Res., 95, 4307–4310, 1990.

Lee, C. C., Liu, J. Y., Reinisch, B. W., Chen, W. S., and Chiu, F. D.: The effects of the pre-reversal drift, EIA asymmetry and magnetic activity on ESF during solar minimum, Ann. Geophys., 23, 745–751, 2005, http://www.ann-geophys.net/23/745/2005/.

Maruyama, T.: A diagnostic model for equatorial spread F 1. Model description and applications to the electric field and neutral wind effects, J. Geophys. Res., 93, 14 611–14 622, 1988.

Maruyama, T. and Matura, N.: Longitudinal variability of annual changes in activity of ESF and plasma depletions, J. Geophys. Res., 89, 10 10 903–10 912, 1984.

Mendillo, M., Baumgardner, J., Xiaoquing, Pi., Sultan, P. J., and Tsunoda, R. T.: Onset conditions for equatorial spread F, J. Geophys. Res., 97, 13 865–13 876, 1992.

Ossakow, S. L.: Spread F theories – A review, J. Atmos. Terr. Phys., 43, 437–452, 1981.

Raghavarao, R., Nageswarrao, M., Sastri, J. H., Vyas, G. D., and Sriramrao, M.: Role of equatorial ionozation anomaly in the initiation of equatorial spread F, J. Geophys. Res., 93, 5959–5964, 1988.

Raghavarao, R., Hoegy, W. R., Spencer, N. W., and Wharton, L.: Neutral temperature anomaly in the equatorial thermosphere- A source of vertical winds, Geophys. Res. Lett., 20, 1023–1026, 1993.

Sahai, Y., Fagundes, P. R., and Bittencourt, J. A.: Transequatorial F-region ionospheric plasma bubbles: solar cycle effects, J. Atmos. Solar Terr. Phys., 62, 1377–1383, 2000.

Sekar, R. and Kelley, M. C.: On the combined effects of vertical shear and zonal electric field patterns on nonlinear equatorial spread F evolution, J. Geophys. Res., 103, 735–755, 1998.

Sekar, R. and Raghavarao, R.: Role of vertical winds on the Rayleigh – Taylor instabilities of the nighttime equatorial ionosphere, J. Atmos. Terr. Phys., 49, 981–985, 1987.

Sridharan, R., Pallam Raju, D., and Raghavarao, R.: Precursor to equatorial spread-F in OI 630.0 nm dayglow, Geophys. Res. Lett., 21, 2797–2800, 1994.

Tsunoda, R. T.: Control of the seasonal and longitudinal occurrence of equatorial scintillation by longitudinal gradients in integrated Pedersen conductivity, J. Geophys. Res., 90, 447–456, 1985.

Whitehead, J.: Ionization disturbances caused by gravity waves in the presence of an electrostatic field and background wind, J. Geophys. Res., 76, 238–241, 1971.

Woodman, R. F. and LaHoz, C.: Radar observations of F region equatorial irregularities, J. Geophys. Res., 81, 5447–5466, 1976.

Zalesak, S. T., Ossakow, S. L., and Chaturvedi, P. K.: Nonlinear equatorial spread F: The effects of neutral winds and background Pedersen conductivity, J. Geophys. Res., 87, 151–166, 1982.